Oncomodulatory properties of the human cytomegalovirus-encoded receptors US28 and UL33

Langemeijer, E.V.

2012

document version
Publisher's PDF, also known as Version of record

chapter 2

HCMV-encoded chemokine receptor US28 modulates oncogenic gene networks: a role for COX-2 in US28-mediated tumor formation

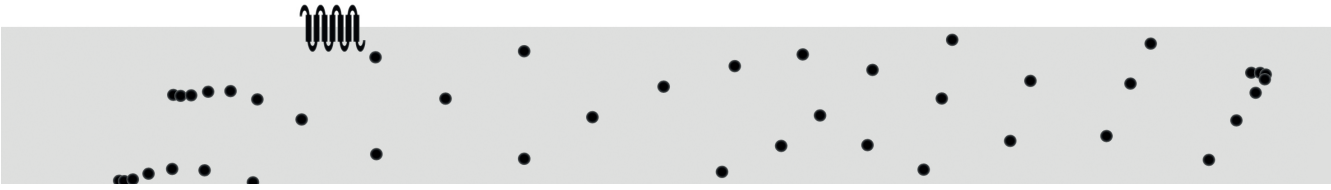

Ellen Langemeijer, David Maussang, Carlos P. Fitzsimons, Marijke Stigter-van Walsum, Remco Dijkman, Martin K. Borg, Erik Slinger, Andreas Schreiber, Detlef Michel, Cornelis P. Tensen, Guus A. M. S. van Dongen, Rob Leurs and Martine J. Smit

Adapted from Canc. Res., ***69****, 2009, 2861-2869*

Abstract

The human cytomegalovirus (HCMV), potentially associated with the development of malignancies, encodes the constitutively active chemokine receptor US28. Previously, we have shown that US28 expression induces an oncogenic phenotype both in vitro and in vivo. Microarray analysis revealed differential expression of genes involved in oncogenic signaling in US28-expressing NIH-3T3 cells. In particular, the expression of cyclooxygenase-2 (COX-2), a key mediator of inflammatory diseases and major determinant in several forms of cancer, was highly upregulated. US28 induced increases in COX-2 expression via activation of NF-κB, driving the production of vascular endothelial growth factor (VEGF). Also in HCMV-infected cells, US28 contributed to the viral induction of COX-2. Finally, the involvement of COX-2 in US28-mediated tumor formation was evaluated using the COX-2 selective inhibitor Celecoxib. Targeting COX-2 in vivo with Celecoxib led to a marked delay in the onset of tumor formation in nude mice injected with US28-transfected NIH-3T3 cells and a reduction of subsequent growth by repressing the US28-induced angiogenic activity. Hence, the development of HCMV-related proliferative diseases may partially be ascribed to the ability of US28 to activate COX-2.

2.1 Introduction

Herpesviruses are widespread pathogens, which establish a life-long latent and persistent infection. In immunocompetent hosts, infection is often asymptomatic while reactivation can lead to serious pathological conditions [184]. In particular, gamma herpesviruses possess oncogenic potential, as they are able to transform cells upon infection [185]. Kaposi's sarcoma-associated herpesvirus (KSHV) is the etiological agent of Kaposi's sarcoma [186], whereas Epstein-Barr virus (EBV) is associated with lymphoproliferative diseases such as Burkitt's lymphoma and Hodgkin's disease [187]. Unlike KSHV and EBV, the human cytomegalovirus (HCMV) is not considered an oncogenic herpesvirus [188], but it has been suggested to act as an oncomodulator [137]. The presence of HCMV proteins has been detected in several malignancies, such as colon cancer [136], malignant glioblastoma [189] and breast cancer [190]. Importantly, HCMV preferably infects tumor cells, leading to enhanced cell proliferation, angiogenesis and resistance to apoptosis [137, 191].

Of interest, most herpesviruses contain one or more genes that encode for constitutively active G-protein coupled receptors (GPCRs) [184]. These viral GPCRs show highest homology to the class of chemokine receptors, known to be involved in the control of the immune system but also the development of various types of cancer [192]. As such, these viral GPCRs likely contribute to viral pathogenesis. The KSHV-encoded GPCR ORF74 is believed to act as a viral oncogene and is considered a key determinant in the pathology of Kaposi's sarcoma. ORF74 possesses proliferative, angiogenic and anti-apoptotic properties, and drives the cell transforming properties of KSHV [5, 102]. Recently, we have shown that the HCMV-encoded chemokine receptor US28, which can bind several chemokines (e.g. CCL2, CCL5, CX3CL1), constitutively activates various inflammatory and proliferative signaling pathways such as NF-κB and induces tumor formation in vivo [6]. Expression of US28 activates $G\alpha_q$-linked signaling pathways, e.g. production of inositol phosphate [82], resulting in an increase in cyclin D1 expression, DNA synthesis and secretion of vascular endothelial growth factor (VEGF) [6]. Mice injected with US28-expressing NIH-3T3 cells develop tumors with high VEGF expression. Moreover, an increase in VEGF promoter activity is also apparent in HCMV-infected glioblastoma cells, which can be attributed to the expression of US28 [6]. Interestingly, US28 expression has also been detected during primary and secondary HCMV infection in immunosuppressed patients [193]. Considering the pathogenic potential of HCMV in these patients, US28 expression at this stage may play a role in the progression of HCMV-linked proliferative diseases.

Profiling of the expression of thousands of genes by means of DNA microarrays has served to discover new oncogenes and potentially new targets for the treatment of cancer [194]. It has also been used to understand molecular mechanisms underlying the development of herpesvirus associated diseases [176, 195, 196]. To gain mechanistic insight into the oncogenic behavior of the HCMV-encoded chemokine receptor US28, we performed microarray analysis on US28 and mock-transfected cells. Various proteins involved in oncogenesis were found to be modulated by the expression of US28. In particular, cyclooxygenase-2 (COX-2) was highly upregulated upon US28 expression. Also in HCMV-infected cells, US28 contributed to the viral induction of COX-2. Finally, the COX-2 specific inhibitor Celecoxib did not only inhibit the upregulation of VEGF in US28-expressing cells, but also markedly decreased US28-induced tumor formation rate in nude mice. As such, US28 upregulates COX-2 expression to promote tumor formation.

2.2 Results

Microarray analysis of US28-expressing cells

Expression of the HCMV-encoded chemokine receptor US28 in NIH-3T3 cells induces increased cell growth and a pro-angiogenic phenotype [6]. To gain insight into the underlying mechanisms of US28-related oncogenic transformation, we analyzed gene expression profiles of US28-expressing NIH-3T3 cells and the corresponding mock-transfected NIH-3T3 cells by cDNA microarray analysis. US28 wild type (WT)-expressing cells showed increases in [^{125}I]-CX3CL1 binding (Figure 2.1A) and inositol phosphate production (Figure 2.1B), which was not apparent in mock-transfected cells. To reproducibly identify differentially expressed genes in our microarray analysis, two independent clonal cell lines, with similar receptor expression and functional characteristics (Figure 2.1A and B) were used for both mock and US28-transfected NIH-3T3 cells. Analysis of the overall microarrays intensities showed highest correlation between biological duplicates (i.e. mock to mock, US28 to US28) (data not shown).

Expression data of the 45,001 Affymetrix probe sets on the Mouse Genome 430 2A Array were normalized (RMA) and analyzed with LIMMA [197]. Using a

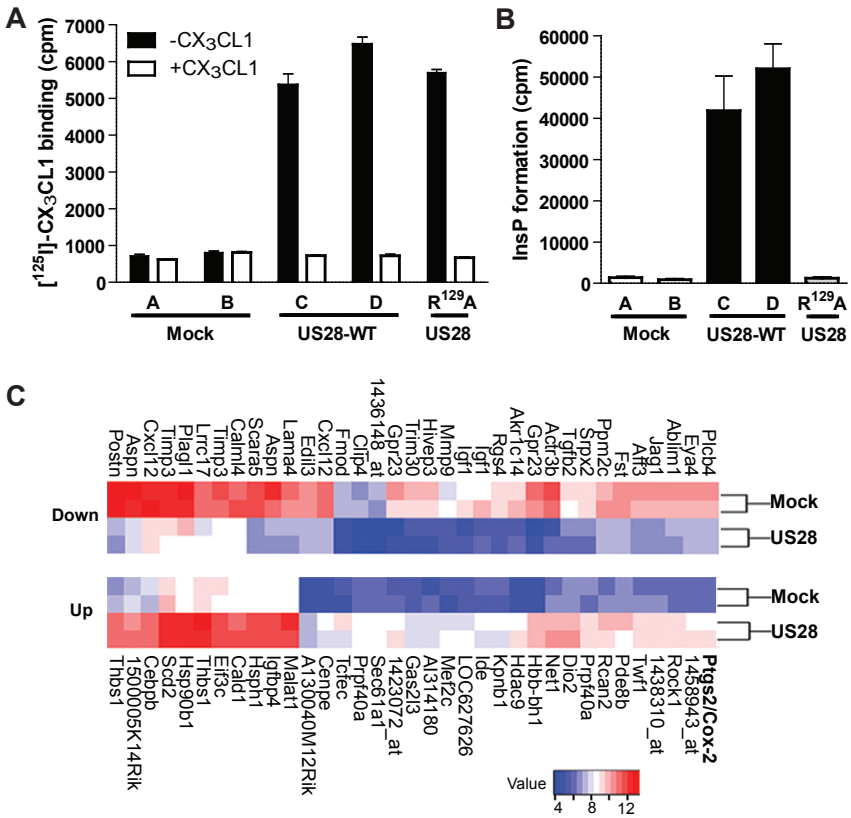

Figure 2.1: Characterization and microarray analysis of US28-expressing NIH-3T3 cells. (A) Independent stable clonal NIH-3T3 cell lines transfected with US28-WT and the G-protein uncoupled mutant US28-R extsuperscript129A bind [^{125}I]-CX3CL1. Unlabelled CX3CL1 displaces specifically bound [^{125}I]-CX3CL1. **(B)** US28-WT constitutively induces the formation of inositol phosphate (InsP), whereas US28-R^{129}A does not. **(C)** Affymetrix Mouse Genome Array data from US28 and mock-transfected cells were analyzed with the LIMMA software using a false discovery rate of 0.02. The 35 most upregulated (Up) and downregulated (Down) probe sets are represented with a heatmap. Colors indicate log^2 intensity values of normalized probe sets.

false discovery rate (FDR) lower or equal to 0.02, we obtained 577 probe sets representing 556 genes (Supplementary Table S1 at http://cancerres.aacrjournals.org/content/69/7/2861/suppl/DC1). The most highly modulated genes are depicted in Figure 2.1C. As can be seen in this figure, the observed changes in gene expression were comparable in the two different clonal mock and US28-expressing cell lines. The involvement of differentially expressed genes in biological pathways was analyzed using DAVID [198] for testing KEGG (Kyoto Encyclopedia of Genes and Genomes) pathways [199]. The 556 genes did not present statistically enriched signaling pathways (after Benjamini correction for multiple testing). Annotation of the genes to the KEGG pathways using the EASE software [200] highlighted pathways involved in focal adhesion, actin cytoskeleton regulation, cell cycle and several forms of cancer, but also signaling pathways such as p53, MAPK, Wnt, and TGFβ (Supplementary Table S2 http://cancerres.aacrjournals.org/content/69/7/2861/suppl/DC1).

To focus on molecular mediators that contribute to the oncogenic potential of US28, we used the CancerGenes resource [201], identifying amongst others, Akt1, Fus, Klf6, Mdm2 and Ptgs2/Cox-2 (Table 2.1). In addition, since US28 has previously been shown to constitutively activate NF-κB signaling pathways [82], the list of modulated genes was compared to known transcriptional targets of NF-κB (adapted from http://jura.wi.mit.edu/young_public/nfkb/literature_targets.xls) (Table 2.1). Ptgs2/Cox-2 also appeared to be one of the most strongly upregulated NF-κB target genes. This finding of Ptgs2/Cox-2 in both cancer and NF-κB gene lists was of particular interest since COX-2 protein is highly upregulated in various forms of cancers [173], but also induced upon HCMV-infection [176].

To validate the microarray expression data, a few genes with high fold changes were analyzed by means of quantitative RT-PCR (qPCR). As observed in the microarray experiment, Ptgs2/Cox-2 as well as other highly differentially expressed genes (Mef2c, Cxcl12 and Tgfb2) showed a similar degree of up or downregulation upon expression of US28 in NIH-3T3 cells (Table 2.2). Because of the previously reported oncogenic potential of US28 in vivo, we also determined expression levels of these genes in RNA extracted from 5 independent US28-induced tumors derived from our xenograft model [6]. Expression of US28 was confirmed in all mouse tumors by qPCR and Ptgs2/Cox-2 mRNA was highly upregulated in US28-induced tumors, highlighting a potential important role for COX-2 during tumorigenesis.

Table 2.1: LIMMA analysis of genes differentially regulated between mock and US28-expressing cells were obtained using a false discovery rate $\leq$ 0.02 (from Supplementary Table S1 http://cancerres.aacrjournals.org/content/69/7/2861/suppl/DC1). The retrieved gene list contained 16 cancer-related genes and 8 NF-κB transcriptional targets. Multiple fold change values represent multiple probe sets available on the array.

Gene symbol	Gene Name	Fold change
CancerGenes resource		
Net1	Neuroepithelial cell transforming gene 1	11,5
Ptgs2/Cox-2	Prostaglandin-endoperoxide synthase 2	6,6
Kpnb1	Karyopherin (importin) beta 1	6,1
Cebpb	CCAAT/enhancer binding protein (C/EBP), beta	10.9, 2.9, 2.2
Actb	Actin, beta	5.1, 3.5, 2.4
Klf6	Kruppel-like factor 6	4.1, 3.3
Cttn	Cortactin	3.4, 3.0
Fus	Fusion (involved in t(12;16) in malignant liposarcoma)	3,5
Runx1	Runt-related transcription factor 1	2,9
Akt1	V-akt murine thymoma viral oncogene homolog 1	2,7
Araf	V-raf murine sarcoma 3611 viral oncogene homolog	2,2
Mdm2	Mdm2, transformed 3T3 cell double minute 2, p53 binding protein (mouse)	2,2
Gli3	GLI-Kruppel family member GLI3	-3,1
Maf	V-maf musculoaponeurotic fibrosarcoma oncogene homolog (avian)	-3,1
Timp3	TIMP metallopeptidase inhibitor 3	-6.3, -9.2
Aff3	AF4/FMR2 family, member 3	-9,8
NF-κB transcriptional targets		
Ptgs2/Cox-2	Prostaglandin-endoperoxide synthase 2	6,6
Hgf	Hepatocyte growth factor	4.9, 4.8, 3.1
Serpine1	Serine (or cysteine) peptidase inhibitor, clade E, member 1	4,2
Nr4a2	Nuclear receptor subfamily 4, group A, member 2	3.8, 3.6, 2.8
Gadd45b	Growth arrest and DNA-damage-inducible 45 beta	2,8
Csf1	Colony stimulating factor 1 (macrophage)	2,6
Cflar	CASP8 and FADD-like apoptosis regulator	2,3
C3	Complement component 3	-2,8
Mmp9	Matrix metallopeptidase 9	-2.8, -6.8
Sox9	SRY-box containing gene 9	-2,9

Table 2.2: Validation of microarray expression data by qPCR in US28-stably transfected NIH-3T3 cells and US28-derived mouse tumors (n=5). Values represent average ± s.e.m. of the fold change in US28-derived samples (cells or tumor) vs mock-transfected cells. Up, upregulated genes; down, downregulated genes.

Modulation	Gene symbol	Microarray	qPCR	
		US28 NIH-3T3 cells	US28 NIH-3T3 cells	US28 mice tumors
	US28		2860 ± 694	475 ± 45
Up	Mef2c	8.9, 2.2, 2.0	5.2 ± 1.2	5.5 ± 0.7
	Ptgs2/Cox-2	6,6	15.8 ± 4.8	22.3 ± 6.3
Down	Cxcl12	10.8, 12.2	33.7 ± 3.1	416.9 ± 96.8
	Tgfb2	6,4	35.3 ± 1.4	238.3 ± 34.0

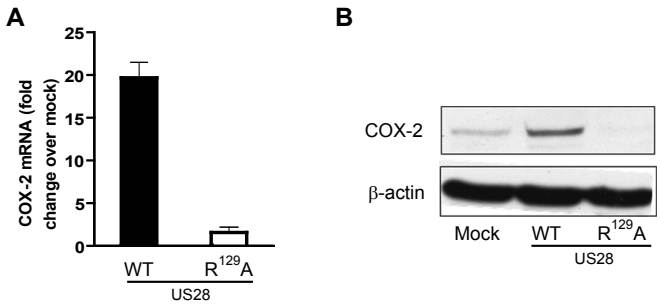

Figure 2.2: US28 constitutively upregulates COX-2 expression. (A) US28-WT-expressing NIH-3T3 cells (filled bar) present higher COX-2 mRNA levels than mock-transfected cells. US28-$R^{129}A$-expressing cells (open bar) do not show any modulation of COX-2 mRNA expression. **(B)** COX-2 protein expression is higher in US28-WT-expressing cells than in mock- and US28-$R^{129}A$-transfected cells.

US28 constitutive activity upregulates COX-2 expression

COX-2 is highly upregulated in a variety of cancers and is known to drive expression of cyclin D1 and VEGF [202]. Since COX-2 is also upregulated in HCMV-infected cells [176] and expression of US28 results in induction of cyclin D1 and VEGF expression [6], we decided to further focus on COX-2 and examine its role in US28-induced proliferative signaling and tumor formation. US28-WT-expressing cells, but not cells expressing the G-protein uncoupled mutant US28-R extsuperscript129A, have been shown to present a transformed phenotype in vitro [6]. NIH-3T3 cells expressing US28-R extsuperscript129A showed comparable receptor expression levels to US28-WT-expressing cells as measured by [125I]-CX3CL1 binding (Figure 2.1A), but did not show increases in inositol phosphate accumulation (Figure 2.1B). Analysis of COX-2 mRNA expression by qPCR showed a 19.7 ± 1.8 fold increase in US28-WT-expressing cells compared to mock-transfected cells (Figure 2.2A). Cells expressing US28-R extsuperscript129A revealed no significant difference (1.6 ± 0.6 fold) in COX-2 mRNA levels compared to mock-transfected cells (Figure 2.2A). Similarly, US28-WT-transfected NIH-3T3 cells showed a marked increase in COX-2 protein expression compared to mock-transfected and US28-R extsuperscript129A-expressing cells (Figure 2.2B).

US28 induces COX-2 and VEGF transcription via activation of NF-κB

In order to understand the molecular mechanisms resulting in the upregulation of COX-2, signaling studies with a COX-2 promoter reporter [203] were performed in HEK 293T cells. US28 induced the human COX-2 promoter activation in a dose-dependent manner, but no increase in COX-2 promoter activity was observed in US28-R extsuperscript129A-expressing HEK 293T (Figure 2.3A). Since the transcription of the COX-2 gene is under the control of NF-κB [204], we investigated the contribution of NF-κB in the COX-2 promoter reporter gene. US28-WT, but not US28-R extsuperscript129A, constitutively activated the NF-κB transcription factor in transfected HEK 293T cells (Figure 2.3A). Moreover, inhibition of NF-κB activation with the IκB phosphorylation inhibitor Bay 11-7082 (5 μM) resulted in a severe reduction of US28-induced COX-2 promoter activation (Figure 2.3B). To further assess the role of NF-κB in the US28-induced COX-2 expression, we used two truncated COX-2 promoter reporter genes that do not contain sequential NF-κB binding sites [203]. 5'-deletions of the distal and both distal and proximal NF-κB binding sites reduced the US28-induced constitutive activation of the COX-2 promoter by respectively 30 and 80% compared to the non-deleted promoter (Figure 2.3C). Since COX-2 is known to drive expression of VEGF [202], shown to be upregulated upon expression of US28 [6], we investigated the role of NF-κB in VEGF promotor activity using the NF-κB inhibitor Bay 11-7082. As seen for the US28-induced COX-2 promotor activity, the US28-induced VEGF promoter activation was markedly inhibited by Bay 11-7082, highlighting the involvement of NF-κB in this process (Figure 2.3D).

US28 induces COX-2 expression in HCMV-infected cells

Infection of cells with HCMV is associated with the activation of various signaling pathways linked to inflammation, including increased expression of COX-2 [177]. Since US28 induced COX-2 expression in transfected cells, we examined the role of US28 in a viral setting. To this end, we used a HCMV deletion virus derived from the AD169 strain that does not contain the sequence encoding for US28 (AD169-ΔUS28). Human foreskin fibroblasts were infected with either mock, AD169-WT or the deletion mutant AD169-ΔUS28 (M.O.I. 3). 8h post-infection (p.i.), only cells infected with the WT virus presented expression of US28 mRNA (Figure 2.4A). As expected, the deletion mutant (Δ) did not induce the expression

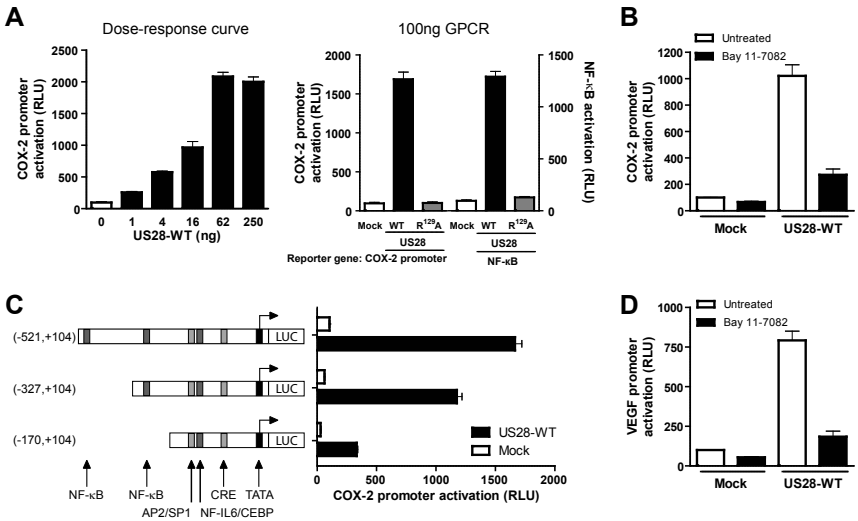

Figure 2.3: US28 activates the COX-2 and VEGF promoters via NF-κB. (A) HEK 293T cells transiently transfected with increasing amounts of US28 show a dose-dependent activation of the human COX-2 promoter luciferase reporter gene. The human COX-2 promoter and the transcription factor NF-κB are activated after transfection of US28-WT, but not with the G-protein uncoupled mutant US28-R^{129}A. **(B)** US28-WT-induced COX-2 promoter activation is inhibited by the NF-κB inhibitor Bay 11-7082 (5μM). **(C)** The US28-WT-induced COX-2 promoter activity is reduced when one and in particular both NF-κB binding sites are removed in 5′-deletion mutants of the human COX-2 promoter. **(D)** US28-WT-induced VEGF promoter activation is inhibited by the NF-κB inhibitor Bay 11-7082 (5μM).

of US28 mRNA. Radioligand binding studies demonstrated that also on the protein level, only cells infected with the AD169-WT virus expressed US28 on their cell surface (Figure 2.4B).

In accordance with earlier findings [177], COX-2 mRNA levels were clearly upregulated in cells infected with the WT virus 8 h p.i., compared to mock-infected cells (Figure 2.4C). In cells infected with AD169-ΔUS28, COX-2 mRNA levels were markedly reduced, highlighting a role for US28 in the viral induction of COX-2. The observed decrease in COX-2 mRNA in AD169-ΔUS28-infected cells was not attributed to impairment in viral IE expression of this mutant strain (data not shown), indicating that the viral replication abilities of both viruses were similar. Since US28 is able to constitutively activate NF-κB [82], we also tested whether this was the case in the HCMV context. Infection of cells with AD169-WT was clearly

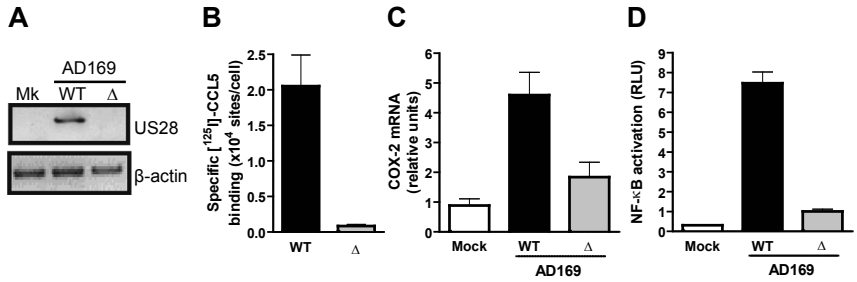

Figure 2.4: US28 mediates COX-2 expression in HCMV-infected cells. (A) Human foreskin fibroblasts infected with mock (Mk), AD169-WT or the deletion mutant AD169-ΔUS28. Viruses only express US28 mRNA with the WT virus 8h p.i. **(B)** [^{125}I]-CCL5 binding shows US28 protein expression in AD169-WT-infected cells, but not in cells infected with AD169-ΔUS28 mutant. **C-D.** Cells infected with AD169-WT present a higher expression level of COX-2 mRNA (**C**) and an increased NF-κB activation (**D**) compared to mock-infected cells. Deletion of US28 gene from the viral genome impairs COX-2 expression and NF-κB transcriptional activity in infected cells.

associated with increased activation of NF-κB as measured using a NF-κB reporter gene (Figure 2.4D). When infecting cells with the US28 deletion mutant, we found that the HCMV-induced NF-κB activation was markedly impaired compared to cells infected with the WT virus (Figure 2.4D). This indicates that upon HCMV infection, US28 activates NF-κB, regulating in turn expression of its transcriptional target COX-2.

COX-2 plays an important role in US28-mediated tumor formation

We have previously shown that US28 upregulates VEGF expression in stably transfected NIH-3T3 cells [6]. Since VEGF expression is in part regulated by COX-2 [202], we tested in vitro the effect of the COX-2 specific non-steroidal anti-inflammatory drug (NSAID) Celecoxib on the US28-induced secretion of VEGF. When culturing US28-expressing NIH-3T3 cells with Celecoxib (25 μM), VEGF secretion was significantly reduced (52 ± 2%, $p<0.001$) indicating the involvement of COX-2 in the US28-induced pro-angiogenic phenotype (Figure 2.5A). As Celecoxib was able to inhibit in vitro an important angiogenic factor involved in US28-induced tumor formation, it was also used in vivo to examine the contribution of

COX-2 during tumorigenesis. Celecoxib treatment was started one day prior to the injection of US28-stably transfected NIH-3T3 cells into nude mice by feeding the animals with chow containing 1500 ppm Celecoxib [205]. As previously described, all control mice injected with US28-expressing cells developed tumors larger than 50 mm3 within 3 weeks. Yet, at this time point, Celecoxib-fed mice showed a severely delayed onset in tumor formation (Figure 2.5B). Developing tumors reached the size of 50 mm3 between 21 and 39 days post-injection, while for the control group, tumor formation occurred between 14 and 21 days post-injection. Celecoxib also increased the tumor doubling time. Untreated mice injected with US28-expressing cells displayed an average tumor doubling time of 3.4 ± 0.3 days, whereas Celecoxib-treated mice presented a longer doubling time of 6.4 ± 0.4 days.

When xenografts had reached their maximum size and animals were sacrificed, no significant changes in VEGF mRNA levels were apparent between the untreated and Celecoxib-treated tumors (data not shown). To measure effects of Celecoxib on the angiogenic activity in US28-induced tumors, we examined CD31 expression by immunohistochemistry. Xenografts derived from stably transfected NIH-3T3 cells lines show highest growth activity in the outer cell layers rather than at the center of the tumor, which can become necrotic when tumors become large. As expected, the angiogenic activity in the untreated US28-derived tumors was clearly apparent in the outer area of the malignancies with a dense localization of CD31 positive blood vessels (Figure 2.5C). Interestingly, the Celecoxib-treated tumors presented a lower staining intensity of CD31 and a less dense distribution of newly formed blood vessels compared to the untreated group. As such, COX-2 inhibition by Celecoxib delayed the onset of US28-induced tumors and slowed their overall growth by repressing angiogenic activity.

2.3 Discussion

Infection of cells with herpesviruses is known to alter cellular gene expression and cell function. Functional genomic analyses of herpesvirus-infected cells have led to the identification of genes that contribute to viral pathogenesis, including induction of tumorigenic events [176, 195, 196]. In view of the reported oncomodulatory potential of HCMV [137] and particularly the observed oncogenic

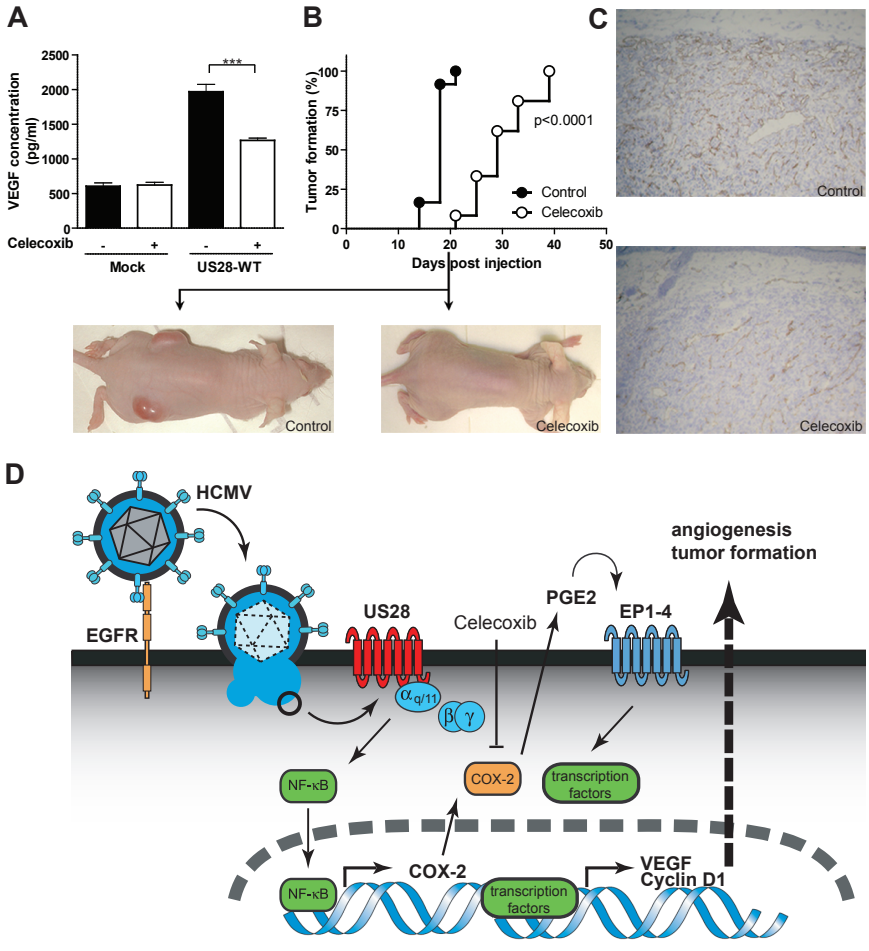

Figure 2.5: Celecoxib impairs US28 oncogenic potential. **(A)** Release of VEGF in the culture medium of US28-stably transfected NIH-3T3 cells is partly inhibited by Celecoxib (25 μM). **(B)** Celecoxib-treated mice injected with US28-expressing cells develop tumors bigger than 50 mm^3 later and at a slower rate than control mice. 20 days post-injection of US28-expressing cells into nude mice, control mice present extensive tumor formation while the Celecoxib-treated group (1500 ppm) is still devoid of tumors. **(C)** Representative CD31 staining in US28-induced tumors from control and Celecoxib-treated mice. **(D)** Schematic representation of US28-induced COX-2 upregulation and role during tumor formation. US28 is expressed at the cell surface of HCMV-infected cells and increases COX-2 expression via NF-κB. COX-2 activity leads to PGE2 release that can bind to its cognate receptors EP1-4 and subsequently induces VEGF and Cyclin D1 transcription. This results in angiogenesis and tumor formation that can be inhibited by Celecoxib. ***, $p<0.0001$.

properties of the HCMV-encoded chemokine receptor US28 [6], we subjected US28-expressing cells to a detailed microarray analysis. As anticipated, US28 and mock-transfected NIH-3T3 cells differentially express genes involved in oncogenic events (e.g. renal cell carcinoma, prostate cancer and melanoma). Significantly modulated genes are implicated in cell cycle, p53 and MAPK pathways (Supplementary Table S2, http://cancerres.aacrjournals.org/content/69/7/2861/suppl/DC1), all associated with proliferation [206-209]. Also, modulation of genes involved in focal adhesion and actin cytoskeleton rearrangement, both of importance in tissue invasion and metastasis [210] is observed. Although these pathways are not statistically enriched in a DAVID analysis, they are correlated to the modulated genes using EASE, providing mechanistic insights on how US28 may induce transformation and tumor development. Another analysis of the microarray data, focusing on cancer-related genes and NF-κB transcriptional targets reveals modulation of genes involved in several forms of cancer that have previously been linked to HCMV infection such as colorectal and breast cancers (Ptgs2/Cox-2, Nr4a2, Serpine1, Csf1 and Gadd45b). Genes participating in multiple forms of cancer (e.g. Net1, Cttn, Runx1, Mdm2, Timp3 and Hgf) are also modulated by US28 expression in NIH-3T3 cells. Although a more systematic approach is required to obtain insight in the oncogenic signaling networks activated by US28, this study points towards several oncogenic targets that are modulated by US28.

Since US28 constitutively activates NF-κB signaling, it is not surprising to observe modulation of NF-κB target genes in US28-expressing cells (Figure 2.1D). One of such genes under control of NF-κB is COX-2 [204], which appears to be highly upregulated in US28-expressing cells and tumors (Table 2.1). COX-2 is of specific interest since it is a key mediator of inflammation and it is now well established that it contributes to the pathogenesis of several forms of cancer. This enzyme is commonly expressed in both premalignant lesions and malignant tumors of e.g. colon, lung, head, neck and breast [173]. In view of the role of COX-2 in tumor development and its upregulation in herpesvirus-infected cells, this enzyme has been suggested to participate in neoplasia induced by some of the oncogenic herpesviruses, including KSHV and EBV [176]. Of interest, HCMV possesses oncomodulatory properties [137] and also upregulates COX-2 expression within a few hours after infection [177].

Since our microarray studies reveal marked increases in COX-2 expression in US28-expressing cells, and US28 was shown earlier to upregulate expression of VEGF and cyclin D1 [6], both known to be regulated by COX-2 [202], COX-2 is a likely determinant in the US28-induced tumor formation. Our studies show that US28 expression is associated with upregulation of COX-2 at both the mRNA and protein levels via activation of NF-κB (Figure 2.2 and 2.3). As expected, NF-κB is

also implicated in the US28-induced VEGF promoter activity (Figure 2.3D). The G-protein uncoupled mutant US28-R^{129}A does not activate NF-κB nor upregulate COX-2 expression (Figure 2.2 and 2.3), indicating a role for G proteins in the US28-mediated COX-2 upregulation [82].

In order to further demonstrate the contribution of COX-2 in the US28-induced tumor formation, we performed *in vitro* assays and intervention studies in our US28 tumor xenograft model using the NSAID COX-2 inhibitor Celecoxib (Figure 2.5). Several clinical studies have provided encouraging evidence of preventive effects of NSAIDs in cancers of colon, lung, breast and prostate [211]. Although some of these drugs were associated with cardiovascular toxicity, recent studies presented Celecoxib as one of the coxibs possessing least side effects [212]. Various animal studies reported effective inhibition of cell growth *in vitro* and tumor growth *in vivo* upon Celecoxib treatment [205, 213, 214]. *In vivo*, Celecoxib treatment of mice injected with US28-expressing cells severely delays and impairs tumor formation. After 3 weeks, no tumors are formed in the Celecoxib-treated mice, while tumors are apparent in the control group, indicating that COX-2 expression is of importance in early tumorigenic events induced by US28. But in the long term, Celecoxib-treated mice also present tumors, indicating that COX-2 is not the sole factor responsible for US28-induced tumor formation. Importantly, Celecoxib treatment reduces the growing rate of the tumor compared to untreated mice ($p<0.001$ in Logrank test), confirming the involvement of COX-2 in tumor development. In addition, Celecoxib impairs the angiogenic phenotype induced by US28, both *in vitro* by significantly ($p<0.0001$) decreasing the production of VEGF in US28-expressing cells, and *in vivo*, by reducing angiogenic activity in US28-derived xenografts. As such, the impairment of the COX-2/VEGF axis by Celecoxib could be accounted for the decreased angiogenesis and subsequent slower development of the tumors *in vivo*. It is important to note that our microarray analysis indicates that other oncogenes beside COX-2 are likely to be implicated in US28-induced tumor progression. The observed inhibitory effect of Celecoxib on tumor formation are most likely attributed to the functional inhibition of COX-2, although some COX-2 independent effects by Celecoxib have been reported [215]. Other targets of Celecoxib include e.g. Cyclin D1 [216] and NF-κB [217], both upregulated in US28-transfected cells. Thus, impairment of US28-induced tumorigenesis by Celecoxib, either through direct or indirect COX-2 inhibition, involves inhibition of proliferative signaling proteins that are constitutively activated by US28.

Cells infected with the AD169 strain devoid of US28 (AD169-ΔUS28) show a reduced activation of NF-κB and upregulation of COX-2 compared to cells infected with the WT virus (Figure 2.4). *In vivo*, US28 expression has been shown in

lung transplant immunosuppressed patients presenting HCMV primary infection or reactivation [193]. Because of the US28-mediated increases in NF-κB activation and COX-2 upregulation in infected cells *in vitro*, US28 may be implicated in virus-associated pathologies by further enhancing and/or contributing to increases in COX-2 expression.

We have previously shown that US28 constitutive activity is mediated by $G\alpha_q$ and $G\beta\gamma$ proteins [6, 82]. The constitutive activation of COX-2 or VEGF promoter by US28 could not be modulated by any of the CC and CX3C chemokines (CCL2, CCL5 and CX3CL1) known to bind this viral GPCR (data not shown). Ligand-stimulation of US28 has however been shown to promote cell migration via activation of $G\alpha_{12/13}$ proteins [158]. As such, the $G\alpha_q$ pathway may be preferentially activated constitutively by US28 during oncogenic transformation, while the ligand-induced signaling may be favorable for the migration of US28-expressing cells. We therefore postulate that upon HCMV infection, US28 is expressed and constitutively activates NF-κB in a ligand-independent manner. US28 potentially activates $G\alpha_q$ and $G\beta\gamma$ [82] to induce the expression of inflammatory proteins such as COX-2 [204]. This enzyme is responsible for the synthesis of PGE2, which through activation of its cognate receptors EP1-4 leads to a subsequent enhancement of cell proliferation (Cyclin D1) and promotion of angiogenesis (VEGF) [202]. US28-dependent increases of at least COX-2 early after infection might be sufficient to catalyze inflammatory processes, which may contribute to or enhance tumor formation (Figure 2.5D). Hence, the development of HCMV-related proliferative diseases might in part be ascribed to the ability of US28 to modulate expression of COX-2.

2.4 Materials and Methods

Cell culture. The mock (empty pcDEF3 expression vector) and US28 stably transfected NIH-3T3 cell lines were cultured as previously described [6]. The human embryonic kidney cell line HEK 293T was cultured in Dulbecco's Modified Eagle's Medium containing 10% fetal bovine serum and transfected using polyethylenimine (PEI). The human foreskin fibroblast BJ cell line was maintained in Minimum Essential Medium (Eagle) with 2 mM L-glutamine and Earle's BSS adjusted to contain 1.5 g/L sodium bicarbonate, 0.1 mM non-essential amino acids, 1.0 mM sodium pyruvate and 10% fetal bovine serum.

Chemokine binding and inositol phosphate accumulation experiments. Stably transfected NIH-3T3 cells and HCMV-infected BJ cells were analyzed for radiolabelled chemokine binding and inositol phosphate formation as previously described [6].

Microarray analysis. NIH-3T3 cells stably transfected with either mock or US28 were serum starved overnight with 0.5% calf serum containing medium. Total RNA was isolated from two independent clones for both cell lines with the RNeasy kit (QIAgen) followed by cDNA synthesis and overnight biotin-labeled cRNA amplification (MessageAmp II aRNA Amplification, Ambion). 20 µg of biotin-labelled cRNA was hybridized to Affymetrix Mouse Genome 430 2.0 arrays and processed according to Affymetrix procedures. Arrays were normalized (RMA) and analyzed using LIMMA statistical package [197]. The data have been deposited in NCBI's Gene Expression Omnibus [218] and are accessible through GEO Series accession number GSE13567 (http://www.ncbi.nlm.nih.gov/geo/query/acc.cgi?acc=GSE13567). Genes differentially expressed between mock and US28-transfected cells were selected based on stringent false discovery rates (FDR $\leq$ 0.02). The retrieved gene lists were analyzed with DAVID and EASE softwares [198, 200] and compared to lists of cancer-related genes (http://cbio.mskcc.org/CancerGenes) and to NF-κB transcriptional targets (adapted from http://jura.wi.mit.edu/young_public/nfkb/literature_targets.xls).

Quantitative real time-PCR (qPCR). For biological validation of microarray data by qPCR analysis, total RNA was isolated from NIH-3T3 cells and from US28 xenografts using the RNeasy kit (QIAgen) and reverse transcribed using iScript cDNA synthesis kit (BioRad), according to the manufacturers' instructions. qPCR primers (from Invitrogen or Isogen) used are described in Table 2.3. PCR reactions were performed using SYBR Green mix with MyiQ Real-Time PCR detection system (Bio-Rad). qPCR on HCMV-infected cells was performed with the ABI-Prism 7700 instrument and the SYBR Green PCR Master Mix (Applied Biosystems). Data were evaluated with the sequence detection software (SDS) version 1.9.1 (Applied Biosystems) and the second derivative maximum algorithm. In addition to melting curve analysis, specificity of the PCR products were confirmed by running controls on agarose gel electrophoresis and subsequent DNA sequence analysis.

Luciferase reporter gene experiments. The NF-κB and VEGF promoter luciferase reporter genes were previously described [6, 82] and the WT and mutated COX-2 promoter luciferase reporter gene plasmids were obtained from Dr Fresno [203]. Luciferase activity was measured 24 h post transfection (RLU, relative light units).

Table 2.3: Sequences of the primers used for quantitative RT-PCR experiments.

Gene symbol	Species	Forward (5'-3')	Reverse (5'-3')
Gapdh	Mus Musculus	TCAACGGCACAGTCAAGG	ACTCCACGACATACTCAGC
Mef2c	Mus Musculus	GGAACACGCCTGTCACCTAAC	TGAATGAGTGCCATACGCCAATG
Cox-2	Mus Musculus	CCTCTGCGATGCTCTTCC	TCACACTTATACTGGTCAAATCC
Tgfb2	Mus Musculus	CTCCACAGTGTTTCAGCCTTTTC	GAACCATCCATCCCAGAAGCC
Cxcl12	Mus Musculus	GGCTCCTTTATCCAGTTCAGTGC	ACAGAGGTGAGAAGCGGAAGTC
US28	HCMV	TGACCGACTACGACTACTTAGAGG	CTGAGCGGGATCACGAAAGC
β-ACTIN	Homo Sapiens	CGGGACCTGACTGACTACCTC	CTCCTTAATGTCACGCACGATTTC
COX-2	Homo Sapiens	GGAGCACCATTCTCCTTGAA	GAAAACCCACTTCTCCACCA
U1A	Homo Sapiens	GCAGCTTATGCCAGGACAGAT	TTGGTGAGGAACAAGATGTGATTC
RPS11	Homo Sapiens	AAGCAGCCGACCATCTTTCA	CGGGAGCTTCTCCTTGCC

Viral experiments. BJ cells were infected with the different HCMV virus strains (AD169-WT and AD169-ΔUS28) [219] with a M.O.I. of 3 and the different assays were performed 8 h post-infection. NF-κB activation was measured by transfecting cells with the NF-κB luciferase reporter gene 24 h before infection.

Western Blot Analysis. Quantification of COX-2 protein level was performed by Western blot on total cell lysates with a rabbit polyclonal COX-2 antibody (Cell Signalling Technology) and a mouse monoclonal β-actin antibody (Sigma).

In vivo experiment. All animal experiments were conducted according to the National Institutes of Health principles of laboratory animal care and Dutch national law ["Wet op de Dierproeven" (Stb 1985, 336)], approved by the Dierexperimentencommissie from the VU Medical Center and performed in compliance with the protocol FaCh 05-02. US28 stably transfected NIH-3T3 cells (2×10^6) were injected s.c. into the flanks of 8 to 10-week-old female nude mice (Hsd, athymic nu/nu, 25–32 g, Harlan Laboratories Cambridge Research Biochemicals). The control group was fed with regular mouse chow (Teklad Harlan), while the Celecoxib group was fed 1 day prior to the cell injection with mouse chow containing 1500 ppm Celecoxib (Pfizer) ad libitum.

Immunohistochemistry. Cryosections of US28-induced xenografts were stained for the presence of CD31 using a rat anti-mouse CD31 antibody (BD PharMingen) with an HRP-conjugated mouse anti-rat antibody (Zymed Laboratories).